Journal of the European Ceramic Society 38 (2018) 5341–5347

Contents lists available at ScienceDirect

Journal of the European Ceramic Society

journal homepage: www.elsevier.com/locate/jeurceramsoc

Original Article

Critical roles of the rhombohedral-phase inducers in morphotropic $NaNbO_3$-$BaTiO_3$-ABO_3 quasi-ternary lead-free piezoelectric ceramics

He Qi[a], Ruzhong Zuo[a,*], Jing-feng Li[b], Longtu Li[b]

[a] Institute of Electro Ceramics & Devices, School of Materials Science and Engineering, Hefei University of Technology, Hefei, 230009, PR China
[b] State Key Laboratory of New Ceramics and Fine Processing, School of Materials Science and Engineering, Tsinghua University, Beijing, 100084, PR China

ARTICLE INFO

Keywords:
Lead-free piezoelectric
MPB
Tolerance factor
$NaNbO_3$

ABSTRACT

A morphotropic phase boundary (MPB) between rhombohedral (R) and tetragonal (T) phases was identified in a few (0.9-x)$NaNbO_3$-0.1$BaTiO_3$-xABO_3 (x = 0–0.05) lead-free systems. Critical roles of R-phase inducers were specially evaluated in terms of phase boundary position, microstructure and piezoelectric responses. The results indicate not only the tolerance factor of the ABO_3 additive but also its ferroelectricity and corresponding volume change would influence the formation of phase boundary and further determine dielectric and ferroelectric responses. The piezoelectric coefficient d_{33} of MPB compositions was compared with theoretically-calculated $d_{33\text{-cal}}$ according to $d_{33} = 2P_r \cdot \varepsilon_{33} \cdot Q_{33}$, demonstrating that the piezoelectric response of these systems should be determined by combined effects of the phase coexistence, nano-scale domains and particularly enhanced dielectric responses. The largest d_{33} ~305 pC/N, the highest $\varepsilon_{33}^T/\varepsilon_o$ ~2815 and the lowest P_r ~14.7 μC/cm^2 were achieved in the MPB composition with 3.75% $SrZrO_3$. These experimental results provide a valuable reference for designing new $NaNbO_3$-based lead-free piezoelectric materials.

1. Introduction

Niobate based lead-free ceramics have attracted increasing attention in the past decade owing to their relatively good dielectric, ferroelectric and piezoelectric properties, particularly for the modulability of their electrical properties through appropriate compositions [1–4]. Unfortunately, the industrial application potentials of (Na,K)NbO_3 (NKN) based ceramics have been seriously challenged by some difficulties in large-scale production and stability issues in properties. The usage of a large amount of highly hygroscopic potassium carbonates and the high volatility of K_2O at high temperatures proves to cause the processing reproducibility and the safety of mass production [5,6]. Most critically, previously reported NKN based lead-free compositions are basically based on a polymorphic phase boundary (PPB) [3], which is attained by simply shifting the temperature regions of three ferroelectric phases such as low-temperature rhombohedral (R) phase, mid-temperature orthorhombic (O) phase and high-temperature tetragonal (T) phase [1,3,7–9]. The PPBs in NKN based systems are generally tilted obviously against the composition coordinate axis in a composition-temperature phase diagram, particularly for some compositions with high piezoelectric coefficient d_{33} values [10,11], and intrinsically differ from traditional morphotropic phase boundaries (MPBs) in Pb(Zr,Ti)O_3 in terms of the nature of coexisting ferroelectric phases [12]. The thermal-driven polymorphic phase transition between R, O or T in NKN-based compositions has intrinsically induced the instability of quasi-static piezoelectric properties owing to the destabilization of poled states during a period of thermal cycling [13–15].

In order to solve above-mentioned issues, $NaNbO_3$ (NN)-based lead and potassium free ceramics have been reported by constructing a quasi-ternary solid solution between NN, $BaTiO_3$ (BT) and $CaZrO_3$ (CZ) [16] /$NaSbO_3$ (NS) [17], in which BT was used as a T-phase inducer, and CZ or NS was used an R-phase inducer. Most importantly, a nearly vertical MPB between T and R ferroelectric phases was discovered, as judged by temperature-independent phase structures (contents) within the phase coexistence zone and temperature-stable piezoelectric and electromechanical coupling properties nearly below their respective T_c values [16,17]. This discovery opens a new way for the device applications of lead-free piezoelectric ceramics because most of piezoelectric sensor and transducer definitely require the thermal stability of small-signal piezoelectric and electromechanical properties. However, it is still unclear what kind of ABO_3 perovskite composition can act as an R-phase inducer in NN-based MPB solid solutions and how they influence the final ferroelectric and piezoelectric properties and the T_c values of near-MPB compositions. It is critical to understand these questions because the magnitude of piezoelectric properties and the temperature range of property stability are especially concerned in the future

* Corresponding author.
E-mail address: piezolab@hfut.edu.cn (R. Zuo).

https://doi.org/10.1016/j.jeurceramsoc.2018.08.034
Received 13 July 2018; Received in revised form 18 August 2018; Accepted 20 August 2018
Available online 22 August 2018
0955-2219/ © 2018 Elsevier Ltd. All rights reserved.

application.

In this work, a few typical lead-free simple perovskites such as $BaZrO_3$ (BZ), $SrZrO_3$ (SZ) and $BiFeO_3$ (BF) as well as CZ and NS with various tolerance factors (τ) were investigated as an R-phase inducer for the construction of NN-BT-ABO_3 system. The purpose to do so is to find out the critical roles of an R-phase inducer in forming interphase boundary and achieving different piezoelectric properties NN-BT-ABO_3 ceramics. Particularly, a universal law of forming the MPB in this lead-free system will be explored. The piezoelectric properties of different MPB compositions were discussed in terms of their crystal symmetry, dielectric and electrostrictive properties.

2. Experimental procedures

The (0.9-x)NN-0.1BT-xABO_3 (NN-BT-xABO_3, ABO_3 = CZ, BZ, SZ, NS and BF, x = 0–0.05) ceramics were prepared by a traditional solid-state reaction method using analytical-grade metal oxides and carbonates as raw materials. The powders were mixed thoroughly in ethanol using zirconia balls for 12 h according to the compositional formula. The mixture was ball-milled again for 24 h after calcination at 900 °C for 5 h, and then pressed into disk samples with a diameter of 10 mm under 100 MPa. The sintering was carried out at 1220–1300 °C for 2 h in air after burning out the binder at 550 °C for 4 h. Silver electrodes were fired on both sides of the polished samples at 550 °C for 30 min. The electroded disks were poled under a dc field of 4 kV/mm for 30 min at room temperature (RT) in a stirring silicone oil bath.

The phase structure of the sample was examined at different temperatures (including RT) by a powder X-ray diffractometer (XRD, D/MAX-RB, Rigaku, Tokyo, Japan) using a Cu Kα radiation (λ = 1.5406 Å). Rietveld refinements on full profiles of XRD patterns were performed by using the program GSAS to identify the crystal symmetry and structural parameters of each phase. The microstructure was observed on the nature surface, and the polished and thermally etched surface of the sintered samples using a field-emission scanning electron microscope (FE-SEM; SU8020, JEOL, Tokyo, Japan). The sample density was measured by the Archimedes method. The domain morphology observation was performed on a transmission electron microscope (TEM) (JEM-ARM200 F, JEOL, Japan). For TEM examination, samples were first mechanically polished to a thickness of ~20 μm and then ion-milled on a Precision Ion Polishing System (PIPS, Model 691, Gatan Inc., Pleasanton, CA) All specimens were annealed at 80 °C for at least one day to release the mechanical stress before the observation. Dielectric properties as a function of temperature and frequency were measured by an LCR meter (Agilent E4980 A, Santa Clara, CA). The polarization versus electric field (P-E) and strain versus electric field (S-E) loops were measured using a ferroelectric test system (Precision multiferroelectric, Radiant Technologies Inc., Albuquerque, New Mexico) connected with an accessory laser interferometer vibrometer (AE SP-S 120E, SIOS Mebtechnils, GmbH, llmenau, Germany). The quasi-static piezoelectric constant d_{33} was measured by a Belincourt-meter (YE2730A, Sinocera, Yangzhou, China) and the planar electromechanical coupling factor k_p was determined by a resonance-antiresonance method with an impedance analyzer (PV70A, Beijing Band ERA Co., Ltd. China).

3. Results and discussion

Fig. 1(a) shows the (200) pseudo-cubic diffraction lines of the RT XRD patterns for NN-BT-xABO_3 ceramics sintered at their optimal temperatures. It can be seen that the 0.9NN-0.1BT (x = 0) ceramic has a T-phase structure owing to the doublet (200) diffraction peak. With increasing x, $(002)_T$ and $(200)_T$ peaks are found to gradually merge together for all of the studied solid-solution systems. A single (200) peak finally appears at a certain value of x, indicating the formation of an R phase. It is interesting to note that the ABO_3 content in MPB compositions differs much from each other, as clearly shown in Fig. 1(b). Relative to other R-phase inducers, a relatively low amount of BF (x = 0.0175) is required to induce an R phase from the T-phase matrix and a relatively high amount of SZ (x = 0.0375) is needed for the same purpose. Lattice instabilities of perovskites are often discussed in terms of the tolerance factor: $\tau = (r_A + r_O)/(\sqrt{2}(r_B + r_O))$, where r_A, r_O, and r_B are the ionic radii of the A, O, and B ions [18]. Generally speaking, an R-distorted unit cell tends to be stabilized for ferroelectric perovskites with lower τ values. This rule is well obeyed for ABO_3 additives such as CZ (τ = 0.914), NS (τ = 0.985) and BZ (τ = 1.004) in the order of $x_{CZ} < x_{NS} < x_{BZ}$ for MPB compositions (see Fig. 1(b)). Compared with CZ and BZ, SZ (τ = 0.947) seems to be a special case. This might be due to the fact that SZ is a distorted perovskite with an orthorhombic symmetry at RT [19]. In addition to the tolerance factor, the ferroelectricity of R-phase inducer plays an additional role in the phase structure transition. BF owns both Fe 3d-O 2p and Bi 6s-O 2p orbital hybridization, favoring lattice instability and octahedral distortion after the substitution of BF for NN [20,21]. Moreover, a relatively obvious shift to low angles can be observed in Fig. 1(a) as NN was substituted by $AZrO_3$ owing to the substitution of larger cations (Na^+:1.39 Å, Ca^{2+}:1.34 Å, Ba^{2+}:1.61 Å, Sr^{2+}:1.44 Å, Nb^{5+}:0.64 Å, Zr^{4+}:0.72 Å), while little shift of diffraction peaks is found in the case of BF and NS (Bi^{3+}:1.36 Å, Fe^{3+}:0.645 Å, Sb^{5+}:0.61 Å). The expansion of the cell volume helps stabilize high-symmetry phases (for example, T phase) [22–24], so that the increasing amount of R-phase inducers is needed in the case of BZ and SZ. Fig. 1(c) shows full XRD patterns of all studied MPB compositions with different x values, indicating all samples exhibit a single perovskite phase without detectable secondary phases although lattice parameters of each composition might be different.

Fig. 2 shows SEM micrographs of various MPB compositions sintered at their optimum temperatures. Fig. 2(a–e) indicates that all samples can be well densified with a high density of more than 95%. Compared with $AZrO_3$ and NS substituted MPB compositions (1270 °C), NN-BT-BF MPB ceramics own a relatively low sintering temperature of 1240 °C and a relatively fine grain morphology probably because BF has a low melting point of ~960 °C. One of the typical features for NKN based ceramics [25] and 0.9NN-0.1BT ceramics [17] is known to have cubic-like grains with sharp edges. As can be seen from Fig. 2(f–j), the addition of the ABO_3 perovskite is found to make the grain edge round in the sintered MPB ceramics, particularly for the case of NS and BF. The sphere-like grain is a common morphology for nearly all Pb-based perovskite piezoelectric ceramics. The modification of grain morphology after adding ABO_3 additives may help the studied lead-free piezoelectric ceramic system own similar processing technology in many aspects as traditional Pb-based perovskite ceramics.

The temperature dependence of the dielectric constant (ε_r) and loss tangent (tanδ) measured at different frequencies for various MPB compositions of each system is shown in Fig. 3(a–e). A diffuse and frequency-dependent dielectric peak can be observed at the temperature of dielectric maxima (T_m) for all samples. The diffuseness degree (γ) and the relaxation degree ($\Delta T_{relax} = T_{m,1\ MHz} - T_{m,1\ kHz}$) were calculated, as marked in the figure of each composition. All studied MPB compositions own a high diffuseness degree (γ = 1.62–1.82). However, there is a big difference in the ΔT_{relax} value for different compositions. It is known that the relaxor behavior is related to the breakdown of the long-range polar ordering as a result of either local random electric fields or local random elastic fields [26]. Comprehensively considering the ionic radius and charge difference, and the substitution content, relatively large ΔT_{relax} and γ values appear in MPB compositions substituted with SZ and BF. Larger ionic charge differences between BF and NN can be mainly responsible for significant dielectric relaxation behavior in BF-substituted NN-BT system although the BF content is lower. By comparison, a relatively high substitution content of SZ dominantly results in obviously enhanced relaxation features in the case of MPB NN-BT-SZ compositions. Furthermore, it can be found that electric poling has produced an irreversible change for all compositions,

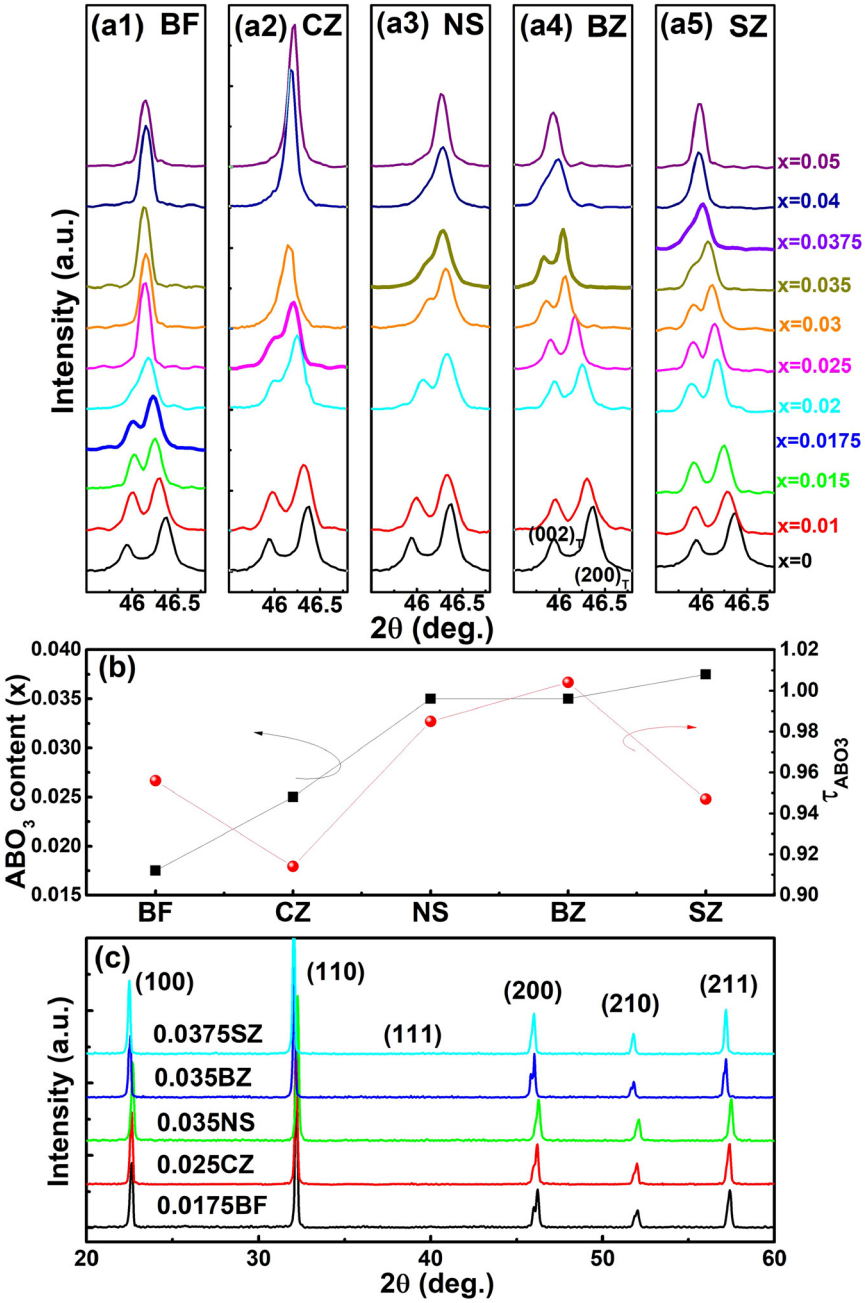

Fig. 1. (a) (200) diffraction lines of XRD patterns at RT for NN-BT-xABO_3 ceramics, (b) the ABO_3 content required for forming MPB and the tolerance factor of ABO_3 phase, and (c) full XRD patterns for NN-BT-xABO_3 ceramics as indicated.

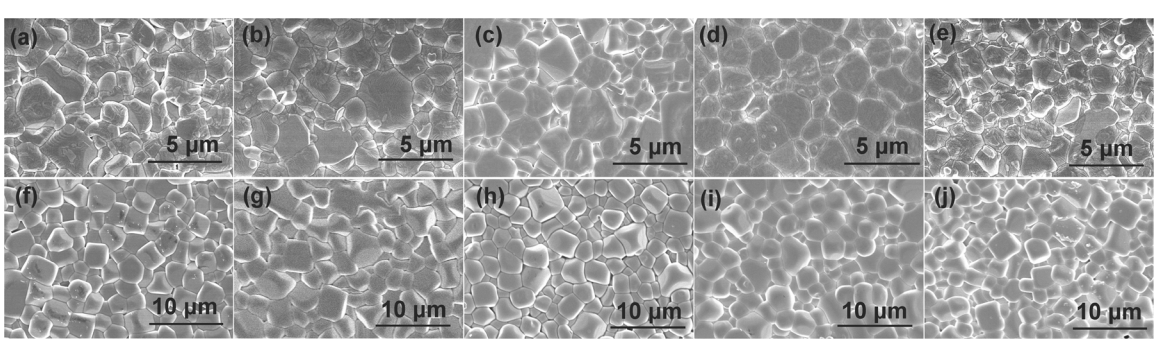

Fig. 2. SEM micrographs on (a–e) polished and thermally etched surfaces and (f–j) as-sintered surfaces of MPB compositions: NN-BT-0.025CZ, NN-BT-0.035BZ, NN-BT-0.0375SZ, NN-BT-0.035NS and NN-BT-0.0175BF, respectively.

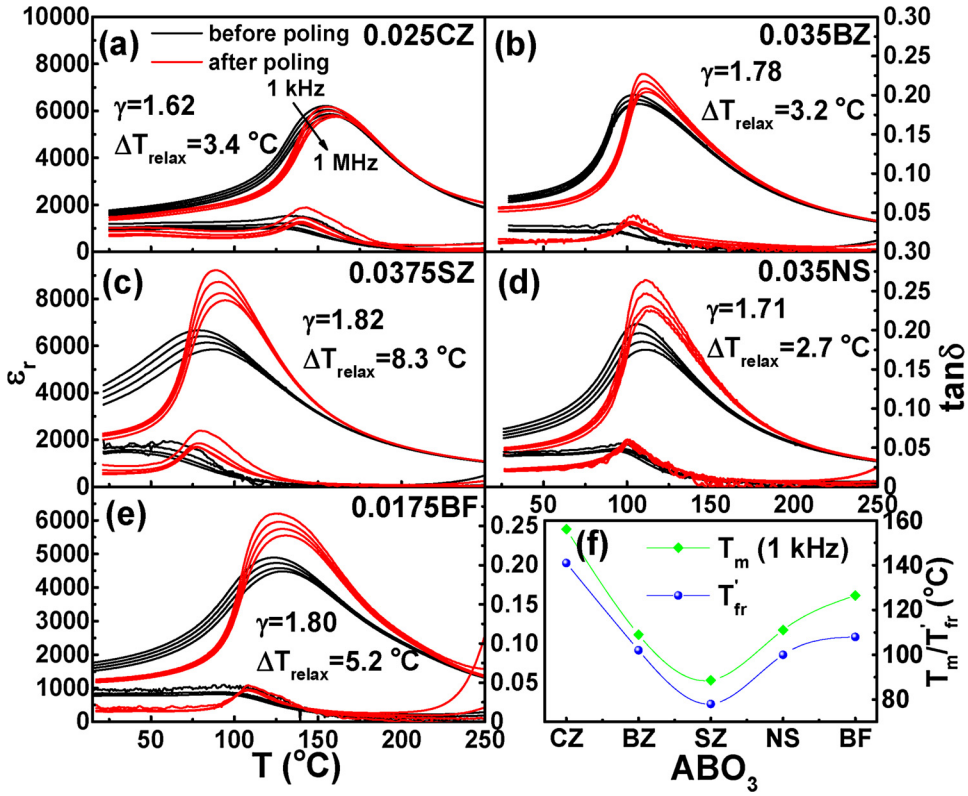

Fig. 3. (a)–(e) Dielectric permittivity and loss tangent measured at various frequencies as a function of temperature for MPB compositions of NN-BT-xABO_3 as indicated, and (f) T_m and T_{fr}' values for MPB compositions as mentioned in (a–e).

as manifested from the appearance of obvious dielectric and loss tangent anomaly peaks at T_{fr}' below T_m. This indicates that all MPB compositions are dominated by a nonergodic relaxor state at RT before poling. Because the nonergodic relaxor state irreversibly changes into a ferroelectric state after poling, the poled samples undergo a phase transition from field-induced ferroelectric state to ergodic relaxor state at T_{fr}' on heating. The T_m and T_{fr}' values for different MPB compositions are summarized in Fig. 3(f). It can be seen that a relatively low T_m (or T_{fr}') and a relatively large RT ε_r (~4300 at 1 kHz) were obtained in the NN-BT-0.0375SZ ceramic.

The Rietveld refinement on full profiles of XRD patterns was performed to identify the crystal symmetry of each phase, as shown in Fig. 4(a) using the NN-BT-0.0375SZ ceramic sample at RT and 75 °C as a representative. The relative content of two coexisting phases in all different samples was identified using the P4mm and R3c as initial modes by means of the multiphase Rietveld refinement of their XRD data. The detailed structural parameters and reliability factors of the NN-BT-0.0375SZ sample at different temperatures up to its T_m are listed in Table 1. The reliability factor of weighted patterns (R_{wp}), the reliability factor of patterns (R_p) and the goodness-of-fit indicator (χ^2) were found to be in the range of 6.44–8.25, 4.82–7.52 and 1.13–1.93, respectively, indicating that the structural model is valid and the refinement result is reliable. As shown in Table 1, an R/T phase coexistence can be observed in a representative system. Particularly, the phase content of coexisting R and T does not change obviously with increasing temperature close to its T_m value, indicating a typical MPB characterization. Moreover, the c/a and volume fraction (F_T) of T phase in each MPB composition as well as the average tolerance factor of MPB compositions are shown in Fig. 4(b). It can be found that the τ difference is quite small for various MPB compositions although the ABO_3 content among them is quite different (see Fig. 1). Fig. 1(b) indicates that in general the ABO_3 phase with larger τ values have less ability to induce the T-R phase transition, so that its content in MPB composition is high. Therefore, one can believe that the τ value of MPB compositions is more or less independent of the phase boundary location, and is roughly 0.976 in the currently studied quasi-ternary lead-free system. On the other hand, the studied MPB compositions, which exhibit optimal piezoelectric properties (see infra), were found to lie at the T-rich side of the phase boundary (the T phase fraction is more than 50%), as observed in some typical Pb-based piezoelectric ceramics [27,28]. Moreover, the NN-BT-0.0375SZ ceramic has relatively low c/a and F_T values compared with other studied MPB compositions, which correspond to its relatively low Curie temperature (see Fig. 3). A relatively small lattice distortion in the NN-BT-0.0375SZ ceramic might help the domain orientation during poling and further enhance piezoelectric response [29,30]. Fig. 4(c) shows the variation of small-signal d_{33} and k_p values as a function of measuring temperature for the NN-BT-0.0375SZ ceramic. It can be seen that both values remain almost constant before its T_m value and rapidly decline thereafter, further supporting the conclusion that the phase coexistence in this study is morphotropic in nature.

Fig. 5(a, b) shows P-E hysteresis loops and butterfly S-E curves for all MPB compositions. The remanent polarization (P_r) and coercive field (E_c) significantly vary from one to another system. These changes might be related to the formation of composition induced dielectric relaxation behavior. The reduction of domain sizes into nanometer scales promotes the reversibility of domain switching upon electric field releasing so that the corresponding P-E loop becomes slimmer. The negative strain (S_{neg}) become smaller simultaneously as observed in S-E curves. As a result, the NN-BT-0.0375SZ ceramic exhibits the smallest E_c and P_r and S_{neg} among all MPB compositions. From S-P^2 curves, one can see an obviously nonlinear behavior at low fields, but a pretty linear relationship at high fields for all compositions, as shown in Fig. 5c. Under a strong electric field, most of domains could be clamped and the influence of domain reorientation would be eliminated, such that the linear increase of polarization merely originates from the ionic displacement at higher fields. By fitting the linear part of S-P^2 curves, one can achieve electrostrictive coefficients Q_{33} of each composition. The

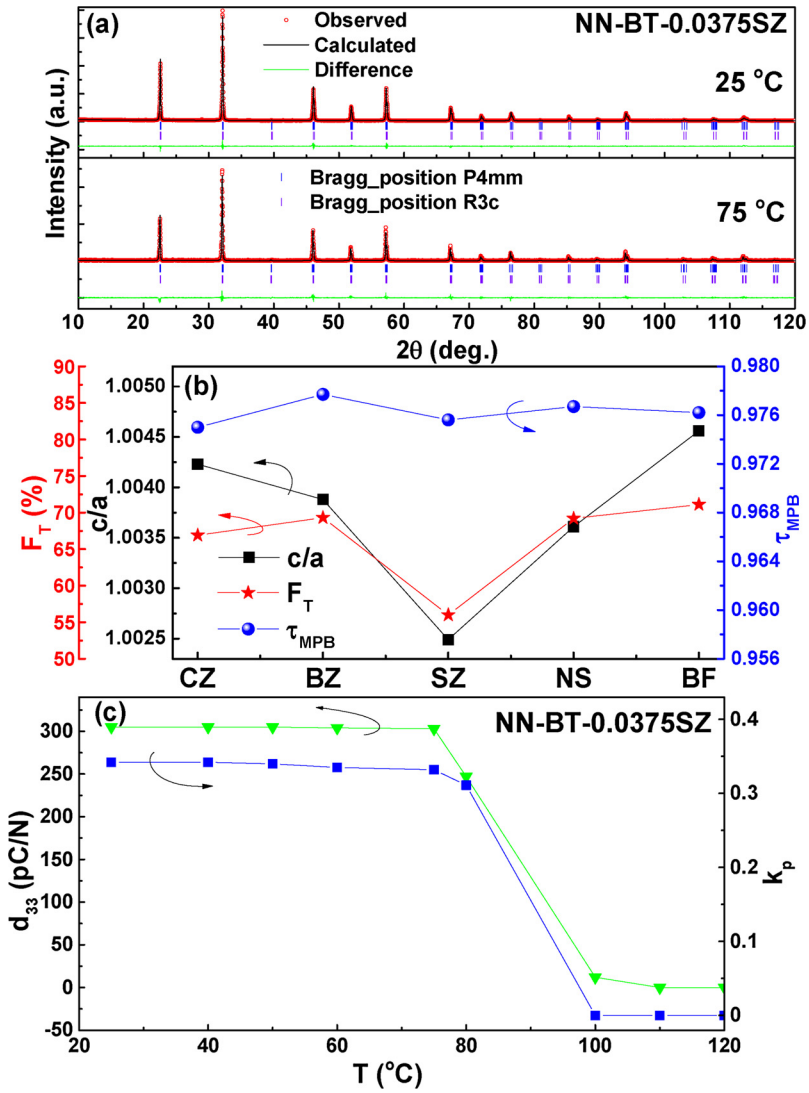

Fig. 4. (a) The Rietveld refinement plots of the NN-BT-0.0375SZ ceramic at 25 °C and 75 °C, (b) the c/a and volume fraction (F_T) of the T phase in different MPB compositions and τ values of various MPB compositions, and (c) temperature dependence of both d_{33} and k_p for the NN-BT-0.0375SZ ceramic.

Q_{33}, d_{33}, P_r and $\varepsilon_{33}^T/\varepsilon_0$ of each MPB composition were listed as a function of the R-phase inducer, as shown in Fig. 3(d). Compared with the 0.9NN-0.1BT binary composition (x = 0, d_{33} = 158 pC/N), all composition systems exhibit significantly enhanced piezoelectric properties close to the MPB. The largest d_{33} value of ~305 pC/N was achieved in the NN-BT-0.0375SZ ceramic. Although the phase coexistence plays a crucial role in the enhancement of piezoelectric responses in MPB piezoelectric ceramics owing to the flattening of the free energy profile, yet an obvious difference in the piezoelectric response of different compositions can be still found for MPB compositions with different additives. It is well known that excellent piezoelectric and electromechanical properties have been found in relaxor ferroelectrics where domain switching during poling becomes much easier because the appearance of polar nano-regions accompanies the

Table 1
Refined structural parameters by using the Rietveld method for NN-BT-0.0375SZ ceramics at different temperatures.

Temperature (°C)	Space group	Volume fraction	Lattice parameters	V (Å^3)	R_{wp} (%)	R_p (%)	χ^2
25	*P4mm*	55%	a = b = 3.9365(1) Å, c = 3.9463(1) Å, α = 90°	61.16	6.44	4.82	1.52
	R3c	45%	a = b = c = 5.5702(5) Å, α = 59.959(4)°	122.21			
40	*P4mm*	57%	a = b = 3.9372(1) Å, c = 3.9472(1) Å, α = 90°	61.19	7.62	5.98	1.16
	R3c	43%	a = b = c = 5.5705(4) Å, α = 59.969(8)°	122.32			
60	*P4mm*	58%	a = b = 3.9374(1) Å, c = 3.9489(1) Å, α = 90°	61.22	7.41	5.19	1.13
	R3c	42%	a = b = c = 5.5733(5) Å, α = 59.973(2)°	122.36			
75	*P4mm*	60%	a = b = 3.9378(1) Å, c = 3.9498(1) Å, α = 90°	61.25	7.89	5.29	1.18
	R3c	40%	a = b = c = 5.5756(5) Å, α = 59.986(1)°	122.45			

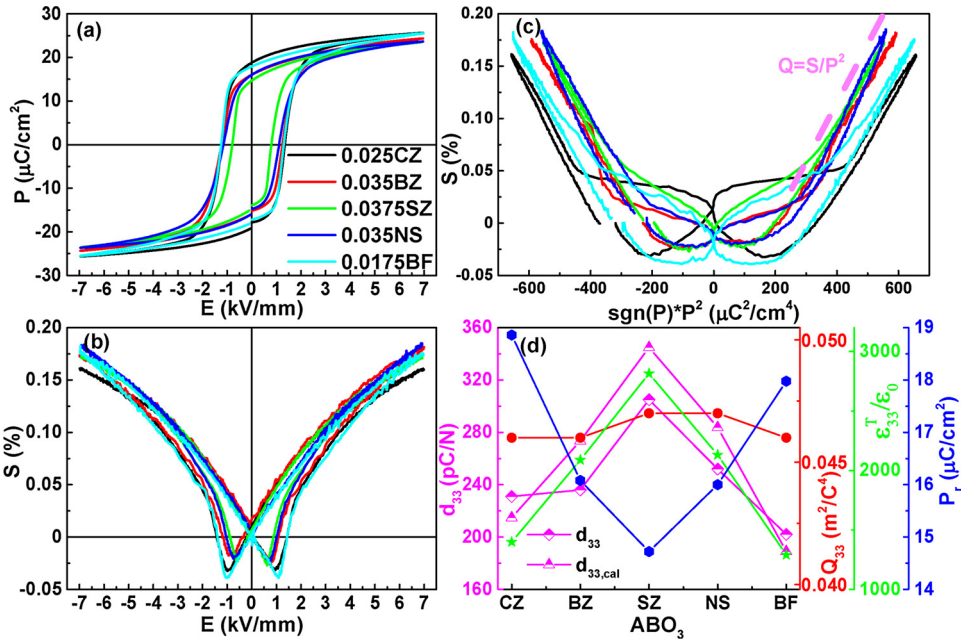

Fig. 5. Bipolar (a) P-E loops, (b) S-E and (c) S-P^2 curves of various MPB compositions, and (d) the quasi-static d_{33}, calculated $d_{33,cal}$, Q_{33}, $\varepsilon_{33}^T/\varepsilon_0$ and P_r of various MPB compositions.

reduction of domain wall energy.

According to the electrostrictive effect, the intrinsic part of d_{33} in perovskite ferroelectrics can be expressed as $d_{33,cal} = 2P_r \cdot \varepsilon_{33} \cdot Q_{33}$, in which d_{33} is the piezoelectric charge coefficient, Q_{33} is the electrostrictive coefficient, and ε_{33} and P_r are the dielectric permittivity and remanent polarization along the polar axis [31]. The calculated $d_{33,cal}$ very much approximates to the quasi-static d_{33} value measured by a d_{33} meter, as shown in Fig. 5(d). As expected, Q_{33} is nearly insensitive to a slight change of additives in NN-BT matrix composition. It is interesting to note that P_r exhibits a completely opposite trend with d_{33}. This is unusual for certain MPB compositions such PZ-PT or PMN-PT where both P_r and d_{33} values usually reach their maxima at the same composition with changing the phase structure because both of them are determined by an irreversible processing after poling. The MPB NN-BT-SZ composition (x = 0.0375) owns the largest d_{33} but the lowest P_r value in all of the studied MPB compositions. It is early to understand that this should be mainly ascribed to the influence of the relaxor properties. The appearance of dielectric relaxation behavior promotes the domain switching, but enhance the dielectric response significantly at the same time. The largest RT dielectric permittivity $\varepsilon_{33}^T/\varepsilon_0 \sim 2815$ was obtained in the composition of NN-BT-0.0375SZ. As a consequence, a large piezoelectric response should be ascribed to the combined effect of the dielectric and ferroelectric responses. Fig. 6 shows the domain morphology of the NN-BT-0.0375SZ sample, in which typical nanoscale R domains (marked as B) and tweed-like T domains (marked as A) are observed [16]. The appearance of polar nano-domains is characteristic of the dielectric relaxation behavior. Moreover, a big difference in dielectric response from different R-phase inducers dominates the deviation of piezoelectric properties for studied MPB compositions. Moreover, the molecular mass difference between A-site and B-site ions should play an important role in electromechanical coupling factors based on the molecular-mass model [32]. Because the substitution content of the ABO_3 phase is very small, the k_p values of the NN-BT-ABO_3 MPB compositions only vary in a narrow range of 0.31-0.34, which are almost in the same magnitude as that of 0.9NN-0.1BT ceramic.

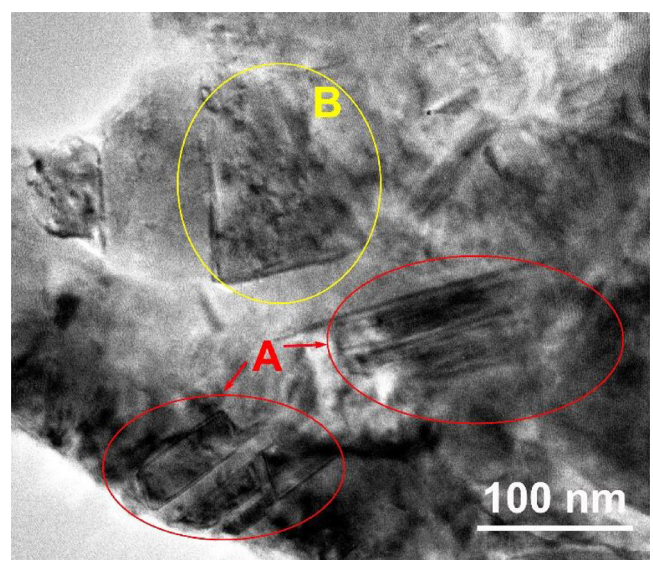

Fig. 6. Bright-field domain morphology of the NN-BT-0.0375SZ ceramic.

4. Conclusions

The dielectric and piezoelectric properties of morphotropic NN-BT-ABO_3 lead-free ceramics were investigated under circumstances of using different R-phase inducers. The phase boundary position, microstructural evolution and piezoelectric response difference in a few solid-solution ceramics were explored to evaluate critical roles of different ABO_3 phases. The amount of ABO_3 phases required for inducing T-R MPB generally rises with increasing the τ value of the ABO_3 perovskite with exceptions of BF and SZ. As an R-phase inducer, the role of the ABO_3 additives should be determined by not only the tolerance factor of a perovskite but also its possible ferroelectricity and the cell volume change. A largest piezoelectric response of $d_{33} = 305$ pC/N was achieved in the MPB composition of NN-BT-0.0375SZ owing to a combined effect of the lowest polarization anisotropy (phase boundary effect), the miniaturization of domains and particularly enhanced dielectric responses.

Acknowledgements

This work was supported by the National Natural Science Foundation of China (Grants No. 51472069, 51332002) and an open fund of the State Key Laboratory of New Ceramic and Fine Processing, Tsinghua University (No. KF201701).

References

[1] Y. Saito, H. Takao, T. Tani, T. Nonoyama, K. Takatori, T. Homma, T. Nagaya, M. Nakamura, Lead-free piezoceramics, Nature 432 (2004) 84–87.
[2] J. Rödel, W. Jo, K.T.P. Seifert, E.M. Anton, T. Granzow, Perspective on the development of lead-free piezoceramics, J. Am. Ceram. Soc. 92 (2009) 1153–1177.
[3] R.Z. Zuo, J. Fu, D.Y. Lv, Phase transformation and tunable piezoelectric properties of lead-free $(Na_{0.52}K_{0.48-x}Li_x)(Nb_{1-x-y}Sb_yTa_x)O_3$ system, J. Am. Ceram. Soc. 92 (2009) 283–285.
[4] P. Li, J.W. Zhai, B. Shen, S.J. Zhang, X.L. Li, F.Y. Zhu, X.M. Zhang, Ultrahigh piezoelectric properties in textured (K,Na)NbO_3-based lead-free ceramics, Adv. Mater. 30 (2018) 1705171.
[5] J. Acker, H. Kungl, R. Schierholz, S. Wagner, R.A. Eichel, M.J. Hoffmann, Microstructure of sodium-potassium niobate ceramics sintered under high alkaline vapor pressure atmosphere, J. Eur. Ceram. Soc. 34 (2014) 4213–4221.
[6] Y.L. Wang, D. Damjanovic, N. Klein, E. Hollenstein, N. Setter, Compositional inhomogeneity in Li-and Ta-modified (K,Na)NbO_3 ceramics, J. Am. Ceram. Soc. 90 (2007) 3485–3489.
[7] J. Fu, R.Z. Zuo, X.Y. Gao, Electric field induced monoclinic phase in $(Na_{0.52}K_{0.48})(Nb_{1-y}Sb_y)O_3$ ceramics close to the rhombohedral-orthorhombic polymorphic phase boundary, Appl. Phys. Lett. 103 (2013) 182907.
[8] G.Z. Zang, J.F. Wang, H.C. Chen, W.B. Su, C.M. Wang, P. Qi, B.Q. Ming, J. Du, L.M. Zheng, Perovskite $(Na_{0.5}K_{0.5})_{1-x}(LiSb)_xNb_{1-x}O_3$ lead-free piezoceramics, Appl. Phys. Lett. 88 (2006) 212908.
[9] D.T. Le, S.J. Kwon, N.R. Yeom, Y.J. Lee, Y.H. Jeong, M.P. Chun, J.H. Nam, J.H. Paik, B.I. Kim, J.H. Cho, Effects of the domain size on local d_{33} in tetragonal $(Na_{0.53}K_{0.45}Li_{0.02})(Nb_{0.8}Ta_{0.2})O_3$ ceramics, J. Am. Ceram. Soc. 96 (2013) 174–178.
[10] K. Xu, J. Li, X. Lv, J.G. Wu, X.X. Zhang, D.Q. Xiao, J.G. Zhu, Superior piezoelectric properties in potassium-sodium niobate lead-free ceramics, Adv. Mater. 28 (2016) 8519–8523.
[11] D.H. Kim, T.G. Lee, S.H. Cho, K.T. Lee, T.H. Lee, Y.W. Hong, C.H. Hong, J.S. Kim, S. Nahm, Piezoelectric properties of $(Na_{0.5}K_{0.5})(Nb_{1-x}Sb_x)O_3$-$SrTiO_3$ ceramics with tetragonal-pseudocubic PPB structure, J. Am. Ceram. Soc. (2018), https://doi.org/10.1111/jace.15542.
[12] B. Jaffe, W.R. Cook, H. Jaffe, Piezoelectric Ceramics, Academic Press, New York, 1971.
[13] R.Z. Zuo, H. Qi, J. Fu, Strain effects of temperature and electric field induced phase instability in (Na,K)(Nb,Sb)O_3-$LiTaO_3$ lead-free ceramics, J. Eur. Ceram. Soc. 37 (2017) 2309–2313.
[14] K. Higashide, H. Kakimoto, Ohsato, Temperature dependence on the piezoelectric property of $(1-x)(Na_{0.5}K_{0.5})NbO_3$–$xLiNbO_3$ ceramics, J. Eur. Ceram. Soc. 27 (2007) 4107–4110.
[15] W.W. Ge, J.F. Li, D. Viehland, Y.F. Chang, G.L. Messing, Electric-field-dependent phase volume fractions and enhanced piezoelectricity near the polymorphic phase boundary of $(K_{0.5}Na_{0.5})_{1-x}Li_xNbO_3$ textured ceramics, Phys. Rev. B 83 (2011) 224110.
[16] R.Z. Zuo, H. Qi, J. Fu, Morphotropic $NaNbO_3$-$BaTiO_3$-$CaZrO_3$ lead-free ceramics with temperature-insensitive piezoelectric properties, Appl. Phys. Lett. 109 (2016) 022902.
[17] H. Qi, H.B. Zhang, R.Z. Zuo, $NaNbO_3$-$BaTiO_3$-$NaSbO_3$ lead and potassium-free ceramics with thermally-stable small-signal piezoelectric properties, J. Am. Ceram. Soc. 100 (2017) 3990–3998.
[18] V.M. Goldschmidt, Die gesetze der krystallochemie, Naturwissenschaften 14 (1926) 477–485.
[19] B.J. Kennedy, C.J. Howard, B.C. Chakoumakos, High-temperature phase transitions in $SrZrO_3$, Phys. Rev. B 59 (1999) 4023.
[20] I. Levin, V. Krayzman, M.G. Tucker, J.C. Woicik, Local structure underlying anomalous tetragonal distortions in $BiFeO_3$-$PbTiO_3$ ferroelectrics, Appl. Phys. Lett. 104 (2014) 242913.
[21] Y. Yoneda, Y. Kitanaka, Y. Noguchi, M. Miyayama, Electronic and local structures of Mn-doped $BiFeO_3$ crystals, Phys. Rev. B 86 (2012) 184112.
[22] Z. Wu, R.E. Cohen, Pressure-induced anomalous phase transitions and colossal enhancement of piezoelectricity in $PbTiO_3$, Phys. Rev. Lett. 95 (2005) 037601.
[23] M. Ahart, M. Somayazulu, R.E. Cohen, P. Ganesh, P. Dera, H.-K. Mao, R.J. Hemley, Y. Ren, P. Liermann, Z.G. Wu, Origin of morphotropic phase boundaries in ferroelectrics, Nature 451 (2008) 545–548.
[24] J.J. Zhou, J.F. Li, X.W. Zhang, Orthorhombic to tetragonal phase transition due to stress release in (Li,Ta)-doped (K,Na)NbO_3 lead-free piezoceramics, J. Eur. Ceram. Soc. 32 (2012) 267–270.
[25] H.C. Song, K.H. Cho, H.Y. Park, C.W. Ahn, S. Nahm, K. Uchino, S.H. Park, H.G. Lee, Microstructure and piezoelectric properties of $(1-x)(Na_{0.5}K_{0.5})NbO_3$-$xLiNbO_3$ ceramics, J. Am. Ceram. Soc. 90 (2007) 1812–1816.
[26] A.A. Bokov, Z.G. Ye, Recent progress in relaxor ferroelectrics with perovskite structure, J. Mater. Sci. 41 (2006) 31–52.
[27] N.G. Luo, Q. Li, Z.G. Xia, X.C. Chu, Phase diagram, temperature stability, and electrical properties of $(0.85-x)Pb(Mg_{1/3}Nb_{2/3})O_3$-$0.10Pb(Fe_{1/2}Nb_{1/2})O_3$-$0.05PbZrO_3$–$xPbTiO_3$ system, J. Am. Ceram. Soc. 95 (2012) 3246–3253.
[28] J. Hur, J.H. Kim, T.G. Lee, I.T. Seo, D.H. Kim, S. Nahm, C.Y. Kang, Structural and piezoelectric properties of $(1-x)Pb(Zr_{1-y}Ti_y)O_3$–$xPb(Zn_{0.4}Ni_{0.6})_{1/3}Nb_{2/3}O_3$ ceramics near triple point, J. Am. Ceram. Soc. 98 (2015) 2887–2893.
[29] Y.S. Sung, J.M. Kim, J.H. Cho, T.K. Song, M.H. Kim, T.G. Park, Roles of lattice distortion in $(1-x)(Bi_{0.5}Na_{0.5})TiO_3$-$xBaTiO_3$ ceramics, Appl. Phys. Lett. 96 (2010) 202901.
[30] T. Leist, T. Granzow, W. Jo, J. Rödel, Effect of tetragonal distortion on ferroelectric domain switching: a case study on La-doped $BiFeO_3$–$PbTiO_3$ ceramics, J. Appl. Phys. 108 (2010) 014103.
[31] S.E. Park, T.R. Shrout, Characteristics of relaxor-based piezoelectric single crystals for ultrasonic transducers, IEEE Trans. Ultrason. Ferroelectr. Freq. Control 44 (1997) 1140–1147.
[32] Y. Yamashita, Y. Hosono, K. Harada, N. Ichinose, Effect of molecular mass of B-site ions on electromechanical coupling factors of lead-based perovskite piezoelectric materials, Jpn. J. Appl. Phys. 39 (2000) 5593–5596.